

1 Inverse correlation between heme synthesis and the Warburg effect in cancer cells

2

3 Yuta Sugiyama¹, Erika Takahashi¹, Kiwamu Takahashi², Motowo Nakajima², Tohru Tanaka², Shun-ichiro

4 Ogura^{1*}

5

6 ¹ School of Life Science and Technology, Tokyo Institute of Technology, Yokohama, Kanagawa, Japan

7 ² SBI Pharma CO., LTD., Roppongi, Tokyo, 106-6020, Japan

8

9 * Corresponding author

10 E-mail: sogura@bio.titech.ac.jp (S.O.)

11 **Abstracts**

12 Cancer cells show a bias toward the glycolytic system over the conventional mitochondrial
13 electron transfer system for obtaining energy. This biased metabolic adaptation is called the Warburg
14 effect. Cancer cells also exhibit a characteristic metabolism, a decreased heme synthesizing ability. Here
15 we show that heme synthesis and the Warburg effect are inversely correlated. We used human gastric
16 cancer cell lines to investigate glycolytic metabolism and electron transfer system toward
17 promotion/inhibition of heme synthesis. Under hypoxic conditions, heme synthesis was suppressed and
18 the glycolytic system was enhanced. Addition of a heme precursor for the promotion of heme synthesis
19 led to an enhanced electron transfer system and inhibited the glycolytic system and vice versa. Enhanced
20 heme synthesis leads to suppression of cancer cell proliferation by increasing intracellular reactive oxygen
21 species levels. Collectively, the promotion of heme synthesis in cancer cells eliminated the Warburg effect
22 by shifting energy metabolism from glycolysis to oxidative phosphorylation.

23 **Introduction**

24 Cancer is caused by accumulation of various genetic mutations. A common feature of most
25 cancer cells is suppression of mitochondrial aerobic respiration and an enhanced glycolytic ATP synthesis
26 for supporting abnormal cellular proliferation and metastasis. Therefore, cancer cells require and utilize
27 abundant glucose and produce excessive lactic acid by accelerated glycolysis, resulting in lactic acidosis
28 [1]. This concept, first advocated by Nobel laureate Otto Warburg in 1924, is widely recognized as the
29 Warburg effect and has pioneered research toward analysis of tumor metabolism.

30 HIF-1 (hypoxia inducible factor 1) is activated owing to low oxygen concentration in cancer
31 cells within the tumor tissue [2–4]. HIF-1 induces pyruvate dehydrogenase kinase-1 (PDK-1), which
32 inactivates pyruvate dehydrogenase (PDH) [5]. PDH is a key player that converts pyruvic acid to acetyl
33 CoA, which links the glycolytic pathway and TCA cycle. Thus, HIF-1 regulates PDK-1 and functions as
34 a modulator of glycolysis and TCA cycle. Moreover, HIF-1 induces glucose transporter-1 and glycolytic
35 enzymes [6,7] and consequently leads to increased lactic acid formation. Thus, HIF-1 shifts metabolism
36 from oxidative phosphorylation to glycolysis under hypoxic conditions [8,9], thereby promoting the
37 Warburg effect under hypoxia.

38 5-Aminolevulinic acid (ALA) is a precursor in the porphyrin synthesis pathway leading to heme
39 formation [10]. The rate-limiting enzyme in heme synthesis is the mitochondrial enzyme ALA synthase

40 (ALAS) [11]. ALA is metabolized to protoporphyrin IX (PpIX) by multiple enzymatic reactions while
41 between cytoplasm and mitochondria, and is finally synthesized into heme by the enzyme ferrochelatase,
42 which coordinates iron ion to porphyrin [12]. Administration of ALA into tumors leads to intracellular
43 accumulation of PpIX because cancer cells exert limited ferrochelatase activity [13,14]. Hypoxia is
44 believed to induce a reduction in PpIX accumulation [15,16]. To the best of our knowledge, the influence
45 of hypoxia on heme synthesis has not yet been clarified [17,18].

46 One of the advantages of the Warburg effect is the ability to suppress cytotoxic reactive oxygen
47 species (ROS), which are produced during aerobic respiration and cause cytotoxicity. Resultantly, cancer
48 cells create a situation favorable for their survival by reducing oxidative stress via suppressing excessive
49 ROS. Recently, attempts have been made to treat cancer by targeting active energy metabolism biased
50 toward cancer glycolysis; for example, studies using dichloroacetic acid (DCA) were reported to induce
51 apoptosis by shifting glucose metabolism from glycolysis to oxidative phosphorylation [19–21].

52 Our previous research using mouse liver showed that ALA increases activity of the
53 mitochondrial enzyme cytochrome *c* oxidase (COX), a rate-limiting enzyme in the electron transport
54 system (ETS) [22]. Owing to the fact that COX is a heme protein, ALA-mediated increase in the amount
55 of heme was thought to induce the expression COX. We also reported that addition of ALA leads to
56 activation of ETS in cancer cells [23].

57 Here we investigated metabolic pathways in cancer cells to understand the relationship between
58 heme synthesis and the Warburg effect. To this end, we comprehensively examined the effect of heme
59 synthesis regulation on energy metabolism in cancer cell lines.

60 **Methods**

61 **Reagents**

62 The substrates 5-aminolevulinic acid (ALA) hydrochloride and succinyl ferrous citrate (SFC)
63 were purchased from Cosmo Bio Co., Ltd. (Tokyo, Japan); 4,6-Dioxoheptanoic acid (Succinylacetone,
64 SA) was purchased from Sigma-Aldrich (St. Louis, MO); and 2,7-Dichlorodihydrofluorescein diacetate
65 (DCFH-DA) and 4,5-dihydroxybenzene-1,3-disulfonate (Tiron) were purchased from Wako Pure
66 Chemical Industries, Ltd. (Osaka, Japan). RPMI-1640 medium and Antibiotic-Antimycotic solution
67 (ABAM, Penicillin-Streptomycin-Amphotericin B mixture) were obtained from Nacalai Tesque (Kyoto,
68 Japan). Fetal bovine serum (FBS) was purchased from Biowest (Nuaille, France).

69

70 **Cell culture**

71 Human gastric cancer cell lines, KatoIII and MKN45, were purchased from RIKEN Bioresource
72 Center (Tsukuba, Japan). Cells were grown in RPMI-1640 medium supplemented with 10% (v/v) heat-
73 inactivated FBS and ABAM and were incubated at 37°C in an incubator with a controlled humidified
74 atmosphere containing 5% CO₂. Cell culture under hypoxic conditions was performed using AnaeroPack-
75 Kenki 5% (Mitsubishi Gas Chemical Co., Tokyo, Japan).

76

77 **Western blot analysis**

78 Western blot analysis was performed as previously described [24]. The following primary
79 antibodies were used: HIF-1 α (sc-10790, 1:400 dilution, rabbit polyclonal, Santa Cruz Biotechnology,
80 Dallas, Texas, USA); GLUT1 (ab652, 1:500 dilution, rabbit polyclonal, Abcam, Cambridge, Great
81 Britain); COX IV-1 (sc-58348, 1:200 dilution, mouse monoclonal, Santa Cruz Biotechnology, Dallas,
82 Texas, USA); and Actin (08691001, 1:200 dilution, mouse monoclonal, MP Biomedicals, Santa Ana,
83 United States). The following secondary antibodies were used: horseradish peroxidase (HRP)-conjugated
84 anti-mouse IgG antibody and HRP-conjugated anti-rabbit IgG antibody (1:3000 dilution, Cell Signaling
85 Technology, Beverly, Massachusetts, USA). HRP-dependent luminescence was developed with Western
86 Lightning Chemiluminescent Reagent Plus (PerkinElmer Life and Analytical Sciences, Inc., Waltham,
87 MA, USA) and detected with a Lumino Imaging Analyzer ImageQuant LAS 4000 mini (GE Healthcare
88 UK, Amersham Place, England).

89

90 **Measurement of glucose uptake**

91 Fluorescent-labeled glucose, 2-NBDG (2-deoxy-2-[(7-nitro-2,1,3-benzoxadiazol-4-yl)]-D-
92 glucose), was used to measure glucose uptake. Cells ($3\sim 8 \times 10^5$ cells/well) were seeded in 6-well plates
93 and preincubated overnight in RPMI-1640 medium in 5% CO₂ gas at 37°C. After changing the culture

94 medium, cells were incubated under each testing condition for 24 hours. Subsequently, all culture medium
95 was removed and replaced with glucose-free culture medium in the presence or absence of fluorescent 2-
96 NBDG (100 μ M). Cells were incubated at 37°C with 5% CO₂ for 25 minutes and washed three times with
97 PBS. Cells were lysed with 0.1 M NaOH and extracted by adding an identical volume of perchloric acid:
98 methanol (1:1, v/v) solution. The obtained mixture was centrifuged to pellet proteins (10,000 \times g, 4°C, 10
99 minutes). The concentration of 2-NBDG in the supernatant was quantitatively determined by measuring
100 fluorescence in a fluorescence spectrophotometer RF-5300 PC (Shimadzu Corporation, Kyoto, Japan).
101 Excitation and emission wavelengths of 465 nm and 550 nm, respectively, were used to measure
102 fluorescence intensity of 2-NBDG. Glucose uptake levels were normalized by intracellular protein levels
103 measured by Bradford protein assay.

104

105 **Measurement of lactate production**

106 Cells were seeded in 96-well plates (2×10^4 cells/well) and preincubated for 2 days in RPMI-
107 1640 medium in 5% CO₂ gas at 37°C. After changing the culture medium to that devoid of FBS, cells
108 were incubated for 24 hours under each testing condition. Lactate production level was measured using a
109 Glycolysis Cell-Based Assay Kit (600450, Cayman Chemical, Ann Arbor, Michigan, USA) according to
110 the manufacturer's protocol.

111

112 **Measurement of pH change in culture medium**

113 Cells were seeded in 35 mm dishes ($3\sim 8 \times 10^5$ cells/well) and preincubated in RPMI-1640
114 medium overnight in 5% CO₂ gas at 37°C. After changing to non-buffering medium containing RPMI-
115 1640 powder medium (Sigma-Aldrich) without sodium bicarbonate, cells were incubated for 24 hours
116 under each testing condition. The pH of the culture medium was measured using a pH meter (LAQUAtwin
117 AS-712, HORIBA, Kyoto, Japan) and the H⁺ concentration was calculated from the pH value. The pH of
118 culture medium without cells was measured as background and the value obtained by subtracting the H⁺
119 concentration of background from the H⁺ concentration of each sample was defined as ΔH^+ . The ΔH^+
120 value was normalized to the intracellular protein concentration.

121

122 **HPLC analysis of porphyrins**

123 Cells were seeded in 6-well plates and preincubated overnight in culture medium. After the
124 culture medium was changed, cells were incubated for 24 hours under each testing condition. They were
125 washed twice with PBS and treated with 0.1 M NaOH. Cellular lysates were prepared by adding 3-fold
126 volumes of dimethyl formamide (DMF)/2-propanol (100:1, v/v) to oxidize coproporphyrinogen III
127 (CPgenIII) to coproporphyrin III (CPIII). CPIII was detected by HPLC because CPgenIII was unstable

128 and easily oxidized. These mixtures were centrifuged to remove proteins, and the supernatants were
129 incubated for a day at room temperature in the dark. HPLC analysis was performed as previously described
130 [25] with some modifications. Briefly, PpIX and CPIII were separated using an HPLC system (Prominence,
131 Shimadzu, Kyoto, Japan) equipped with a reversed-phase C18 Column (CAPCELL PAK, C18, SG300, 5
132 μm , 4.6 mm \times 250 mm, Shiseido Co., Ltd., Tokyo, Japan). Elution was started with 100% solvent A and
133 0% solvent B for 5 minutes, with a linear gradient of solvent B (0%–100%) for 25 minutes and later with
134 solvent B for 10 minutes. Flow was maintained at a constant rate of 1.0 mL/min. Porphyrins were
135 continuously detected using a fluorospectrometer (excitation 404 nm; emission 624 nm). Porphyrin
136 concentration was estimated using calibration curves constructed using porphyrin standards.

137

138 **HPLC analysis of intracellular heme level**

139 Cells were seeded in 35-mm dishes and preincubated overnight in culture medium. After the
140 culture medium was changed, they were incubated for 24 hours under each testing condition. Cells were
141 washed three times with PBS and treated with 0.1 M NaOH on ice. Elution solvent A contained 1 M
142 ammonium acetate and 12.5% acetonitrile (pH 5.2), and solvent B contained 50 mM ammonium acetate
143 and 80% acetonitrile (pH 5.2). Cellular lysates were prepared by adding 3-fold volumes of elution solvent
144 A/solvent B (1:9, v/v) to extract intracellular heme. These mixtures were centrifuged to remove proteins

145 (10,000 × g, 4°C, 10 minutes), and the supernatants were collected. Heme was measured using an HPLC
146 system (Prominence, Shimadzu, Kyoto, Japan) equipped with a reversed-phase C18 Column (CAPCELL
147 PAK, C18, SG300, 5 μm, 4.6 mm × 250 mm, Shiseido Co., Ltd., Tokyo, Japan). Elution was maintained
148 with 10% solvent A and 90% solvent B for 7 minutes. Flow was maintained at a constant rate of 2 mL/min.
149 Heme was continuously detected by absorbance at 404 nm using a spectroscopic detector. Heme
150 concentrations were estimated using calibration curves constructed using heme standard.

151

152 **Measurement of COX activity**

153 Measurement of cytochrome *c* oxidase (COX) activity was performed as previously described
154 with some modifications [22]. Mitochondrial fractions were obtained using a Mitochondria Isolation Kit
155 (MITOISO2, Sigma-Aldrich). Briefly, 5×10^7 cells were washed and homogenized in extraction reagent.
156 The homogenate was centrifuged at $600 \times g$ for 5 minutes and the supernatant was centrifuged further at
157 $11,000 \times g$ for 10 minutes. The pellet was suspended in storage buffer and used as the mitochondrial
158 fraction. Protein concentrations were determined by the Bradford assay (Bio-Rad Laboratories, CA). COX
159 activity was measured using a Cytochrome *c* Oxidase Assay Kit (Sigma-Aldrich). Briefly, 100 μg of the
160 mitochondrial fraction was diluted with enzyme dilution buffer containing 1 mM n-dodecyl β-d-maltoside.
161 Ferrocyanochrome *c* (reduced cytochrome *c* with dithiothreitol) was added to the sample, and COX activity

162 was measured by the decrease in absorption at 550 nm. The difference in extinction coefficients between
163 reduced and oxidized cytochrome *c* is 21.84 at 550 nm [26]. One unit of COX activity was defined as the
164 oxidization of 1.0 μ mole of ferrocytochrome *c* per minute at pH 7.0 at 25°C.

165

166 **Determination of mitochondrial DNA copy number**

167 Genomic DNA was isolated using the NucleoSpin® RNA II and NucleoSpin® RNA/DNA Buffer
168 Set kit (MACHEREY-NAGEL, Düren, Mannheim, Germany) kit according to the manufacturer's
169 instructions. Quantitative real-time PCR was performed with SYBR Premix Ex Taq (TaKaRa, Shiga,
170 Japan) using Thermal Cycler Dice® Real Time System Single (TaKaRa, Shiga, Japan) to determinate the
171 amount of mitochondrial DNA (mtDNA) content relative to the nuclear DNA (nuDNA). Primer sets were
172 as follows; human mtDNA, forward 5'-CACCCAAGAACAGGGTTTGT-3' and reverse 5'-
173 TGGCCATGGGTATGTTGTTA-3'; human nuDNA, forward 5'-
174 TGCTGTCTCCATGTTTGATGTATCT-3' and reverse 5'-TCTCTGCTCCCCACCTCTAAGT-3'. The
175 PCR amplification conditions included 95°C for 30 seconds; 50 cycles at 95°C for 5 seconds and 60°C for
176 60 seconds each; dissociation for at 95°C for 15 seconds and at 60°C for 30 seconds; and at 95°C for 15
177 seconds on a Thermal Cycler Dice Real-Time System. Thermal Cycler Dice Real-Time System analysis
178 software (TaKaRa, Shiga, Japan) was used for data analysis. The Ct values (cycle threshold) were

179 calculated using the crossing-point method, and the relative mtDNA and nuDNA levels were measured by
180 comparison with a standard curve. The mtDNA content was normalized with the content of nuDNA.

181

182 **Cell growth assay**

183 MKN45 cells (8×10^4 cells) were incubated overnight at 37°C in 5% CO₂ in RPMI-1640
184 medium. The culture medium was changed to fresh medium containing 1 mM ALA, 0.5 mM SFC, and/or
185 100 μM Tiron and cultured for up to 4 days in 5% CO₂ in dark. Cells were collected after trypsin treatment,
186 and the number of living cells was determined using trypan blue dye exclusion assay.

187

188 **Detection of reactive oxygen species**

189 ROS detection assay was performed using the cell-permeable fluorogenic probe DCFH-DA.
190 Briefly, DCFH-DA diffuses into cells and is deacetylated by cellular esterase to DCFH, which is rapidly
191 oxidized to highly fluorescent DCF by ROS. The fluorescence intensity of DCF can be assessed as an
192 indicator of cellular ROS levels.

193 MKN45 cells were incubated with 1 mM ALA, 0.5 mM SFC, and/or 100 μM Tiron for 24 hours.
194 After washing with PBS, the media was changed to serum-free medium supplemented with 10 μM DCFH-
195 DA. After incubating for 30 minutes, the medium was discarded and cells were collected by a cell scraper

196 using 200 μ L of Hanks' balanced salt solution (HBSS) (-). The collected solution was suitably diluted
197 with HBSS (-) and the fluorescence was measured using a spectrophotometer F-7000 (Hitachi High-Tech
198 Science, Tokyo). DCF fluorescence intensity was detected at an excitation wavelength of 480 nm and a
199 fluorescence wavelength of 525 nm.

200

201 **Statistical analysis**

202 Data are expressed as means \pm standard deviation using two or three independent experiments.

203 Data were analyzed for statistical significance using Student's t-test for the comparison between the

204 control and experimental groups. Difference was assessed with two-sided test with an α level of 0.05. In

205 case of three or more groups, statistical significance was analyzed using the Dunnett's test or Tukey-

206 Kramer's test with an α level of 0.05. Statistical analyses were performed using the JMP[®] 13 software

207 (SAS Institute Inc., Cary, NC, USA).

208 **Results**

209 **Glycolytic increase in gastric cancer cells under hypoxia**

210 We examined the gastric cancer cell lines KatoIII and MKN45 to understand the relation
211 between glycolysis and heme synthesis under hypoxia. Under hypoxic conditions, cancer cells induce
212 expression of the glucose transporter GLUT1 and increase glucose uptake via HIF-1, thereby resulting in
213 excessive lactic acid production and shifting the acid-base equilibrium toward the acidic side [6].
214 Therefore, we assessed the functional status of the glycolytic system by measuring the expression of
215 GLUT1, uptake of a fluorescent glucose analog, 2-NBDG, lactic acid concentration, and pH of the culture
216 media.

217 The cell lines were cultured for 24 hours under normoxic (21% O₂) or hypoxic (1% O₂)
218 conditions. On performing expression analysis, in both cell lines, the expression of GLUT1 was found to
219 be enhanced by HIF-1 α under hypoxic conditions (Fig 1A). In correlation with up-regulated GLUT1, the
220 uptake of 2-NBDG was significantly increased under hypoxic conditions (Fig 1B). Moreover,
221 concentrations of lactic acid concentration (Fig 1C) and H⁺ concentration (Fig 1D) were also significantly
222 increased. Thus, hypoxic conditions accelerated glycolysis in gastric cancer cell lines. These experiments
223 also served to confirm their application in evaluating the glycolytic system.

224

225 **Fig 1. Hypoxia enhances glycolysis in human gastric cancer cell lines.** KatoIII and MKN45 cells were
226 used for experiments following incubation either under normoxia (21% O₂) or hypoxia (1% O₂) for 24
227 hours. (A) HIF-1 α and GLUT1 were detected by Western blotting. (B) Glucose uptake was assessed after
228 incubation for 25 minutes with 100 μ M 2-NBDG. (C) Extracellular lactate concentration and (D) change
229 in pH of medium was measured. Values are means \pm SD, n = 3, Asterisk indicates a significant difference
230 (*; $p < 0.05$, **; $p < 0.01$).

231

232 **Reduction of intracellular PpIX and heme levels in gastric cancer** 233 **cells under hypoxic conditions**

234 Previous studies have shown that under hypoxic conditions, the accumulation of PpIX reduces
235 when ALA is supplemented [15,16]. However, the effect of hypoxia on porphyrin synthesis or
236 accumulation, without ALA supplementation, has not yet been clarified. Therefore, we measured the
237 amount of the porphyrin in gastric cancer cell lines by high-performance liquid chromatography (HPLC)
238 after culturing for 24 hours under normoxic (21% O₂) or hypoxic (1% O₂) conditions. The amount of
239 intracellular PpIX in both KatoIII and MKN45 cells was reduced under hypoxic conditions (Fig 2A),
240 whereas extracellular coproporphyrin III (CPIII) was remarkably increased (Fig 2B). Conversely, no other
241 type of porphyrin was detected intra- or extra-cellularly. Thus, under hypoxic conditions, the porphyrin

242 synthesis pathway is thought to be inhibited at the CPgenIII step resulting in excretion of the synthesized
243 CPgenIII and decrease in PpIX. The amount of intracellular heme under hypoxia was also measured by
244 HPLC after culture for 24 hours under normoxic (21% O₂) or hypoxic (1% O₂) conditions (Fig 2C). A
245 significantly reduced intracellular heme concentration indicated inhibitory effect of hypoxia on heme
246 synthesis. This also supported the hypothesis that the porphyrin synthesis pathway is inhibited at the
247 CPgenIII step under hypoxia. Thus, we can postulate a negative correlation between heme synthesis and
248 the glycolytic system.

249

250 **Fig 2. Hypoxia leads to excretion of the heme-intermediate CPIII and reduction of heme content in**
251 **human gastric cancer cell lines.** KatoIII and MKN45 cells were incubated under normoxia (21% O₂) or
252 hypoxia (1% O₂) for 24 hours and intracellular PpIX (A), extracellular CPIII (B) and intracellular heme
253 concentration (C) were measured. Other porphyrins were not detected. Values are means ± SD, n = 2 (A,
254 B) and n = 3 (C), Asterisk indicates a significant difference (*; $p < 0.05$, **; $p < 0.01$).

255

256 **Inverse correlation between heme biosynthesis and glycolysis**

257 Next, we examined the effect of heme synthesis on glycolysis in cancer cell lines using ALA,
258 SFC as iron ion, and SA. The addition of ALA and iron ion promotes heme synthesis because the rate-

259 limiting step in PpIX production is ALA synthesis and heme formation by coordination of divalent iron
260 ions to PpIX [11]. Conversely, SA suppresses heme synthesis by inhibiting ALA dehydratase, which
261 functions in condensing two molecules of ALA.

262 The gastric cancer cell lines were cultured for 24 hours in media containing 1 mM ALA, 0.5
263 mM SFC, or 0.5 mM SA, followed by measurement of intracellular heme by HPLC. The addition of ALA
264 alone or ALA+SFC induced an increase in intracellular heme concentration, whereas SA led to its
265 reduction (Fig 3A). Thus, heme synthesis can be regulated by the addition of ALA, SFC, or SA.

266 Next, we tested the effect of heme synthesis on glycolysis by analyzing the uptake of 2-NBDG,
267 lactic acid concentration, and H^+ concentration after 24 hours of cell culture with 1 mM ALA, 0.5 mM
268 SFC, or 0.5 mM SA. Under conditions that enhanced heme synthesis (i.e., supplementation with ALA or
269 ALA+SFC), the uptake of 2-NBDG was similar or reduced compared with control (Fig 3B). Conversely,
270 the uptake of 2-NBDG was significantly higher under conditions that suppressed heme synthesis (SA).
271 Lactic acid concentration in MKN45 cells was down-regulated by supplementation of ALA or ALA+SFC
272 and up-regulated by addition of SA (Fig 3C). However, no such difference was observed in KatoIII cells.
273 Furthermore, both cell lines showed a tendency toward decrease in H^+ concentration upon addition of
274 ALA+SFC (Fig 3D). H^+ concentration in KatoIII cells was increased after supplementation with SA (Fig
275 3D). Thus, heme synthesis and glycolysis are inversely related in gastric cancer cell lines.

276

277 **Fig 3. Heme synthesis is inversely correlated with glycolysis.** KatoIII and MKN45 cells were used for
278 experiments following incubation with 1 mM ALA, 0.5 mM SFC and 0.5 mM SA for 24 hours. (A)
279 Intracellular heme concentration measured by HPLC. (B) Glucose uptake assessed after 25 minutes of
280 incubation with 100 μ M 2-NBDG. (C) Extracellular lactate concentration and (D) change in pH of medium
281 was measured. Values are means \pm SD, n = 3, Asterisk indicates a significant difference analyzed by
282 Dunnett's test (*; $p < 0.05$, **; $p < 0.01$).

283

284 **Correlation between heme synthesis and mitochondrial activity**

285 COX, a heme protein, is the rate-limiting enzyme of the mitochondrial electron transfer chain
286 [27,28]. Injection of ALA induced expression and activity of COX in mice liver [22]. It also enhanced
287 COX expression and oxygen consumption in a lung cancer cell line, A549 [23]. Accordingly, we expected
288 that regulation of heme synthesis using ALA, SFC, and SA should affect mitochondrial activity.

289 First, we examined the expression of COX to investigate the effect of heme synthesis regulation
290 on mitochondrial activity. We evaluated the expression of COX IV-1, the nuclear-encoded largest subunit
291 of COX and isoform expressed under normal conditions [29], in cancer cells after incubation for 24 hours
292 with ALA, SFC, and SA (Fig 4A). COX expression increased in both cell lines when heme synthesis was

293 enhanced by ALA or ALA+SFC. In contrast, COX expression was reduced in MKN45 cells when heme
294 synthesis was suppressed by SA. Analysis of COX activity in MKN45 cells revealed significant elevation
295 upon ALA and ALA+SFC supplementation and reduction after SA supplementation (Fig 4B). These
296 results indicate that the expression (Fig 4A) and enzyme activity of COX increased when heme synthesis
297 was promoted and decreased when it was suppressed. Enhanced heme synthesis after addition of
298 ALA+SFC led to up-regulation of COX, most probably because it is a hemoprotein. It can thus be
299 predicted that SA-mediated suppression of heme synthesis would probably reduce COX expression and
300 activity.

301 Second, we measured the copy number of mitochondrial DNA (mtDNA) (Fig 4C). Genomic
302 DNA was extracted from MKN45 cells after cell culture for 24 hours under each testing condition (1 mM
303 ALA, 0.5 mM SFC, and 0.5 mM SA). Quantitative real-time PCR was performed to determinate the
304 amount of mtDNA relative to the nuclear DNA (nuDNA). The mtDNA copy number increased upon
305 supplementation of ALA+SFC and decreased after addition of SA. Thus, mitochondrial concentration can
306 be correlated with enhanced heme synthesis.

307

308 **Fig 4. Heme synthesis is positively correlated with COX expression and mtDNA copy number. (A)**

309 Expression of COX IV in KatoIII and MKN45 cells was detected by Western blotting after incubation

310 with 1 mM ALA, 0.5 mM SFC, and 0.5 mM SA for 24 hours. (B) MKN45 cells were incubated with 1
311 mM ALA, 0.5 mM SFC, and 0.5 mM SA for 24 hours; the cells were then harvested and COX activity
312 was measured. (C) Relative copy number of mitochondrial DNA (mtDNA) versus nuclear DNA (nuDNA)
313 of MKN45 cells was determined by real-time PCR. Cells were treated with 1 mM ALA, 0.5 mM SFC, and
314 0.5 mM SA for 24 hours before the test. The relative mtDNA copy number of the control is shown as 1 in
315 the graph. Values are means \pm SD, n = 3 (B) and n = 2 (C), Asterisk indicates a significant difference
316 analyzed by Dunnett's test (*; $p < 0.05$, **; $p < 0.01$).

317

318 This further indicated a positive correlation between synthesis of heme and activity of
319 mitochondria, including that of COX. Thus, enhanced heme synthesis is suggested to resolve the Warburg
320 effect by increasing COX activity and vice versa.

321

322 **Inhibition of cancer proliferation via ROS by promoting heme** 323 **synthesis**

324 Next, we examined the proliferation of cancer cells under conditions where heme synthesis was
325 enhanced and the Warburg effect was eliminated. MKN45 cells were cultured with ALA and/or SFC for

326 4 days, following which the number of cells was counted (Fig 5A). Addition of ALA and ALA+SFC led
327 to suppression of cell proliferation to <50% compared with the control group.

328 Mitochondria, the seat of oxidative phosphorylation, are also the main source of ROS generation
329 [30,31]. The amount of ROS was measured to investigate the increased COX activity upon addition of ALA (Fig 5B).
330 The changes in the amount of ROS were also determined when Tiron was added as a ROS scavenger
331 [32,33]. ROS increased significantly after addition of ALA and/or SFC and was markedly suppressed
332 under conditions where Tiron was added. MKN45 cells were cultured with ALA, SFC, and Tiron for 4
333 days and the growth was measured (Fig 5C). The ALA+SFC-mediated suppression of cell growth was
334 significantly neutralized by Tiron. Thus, the proliferation of cancer cells was suggested to be suppressed
335 by intracellular ROS caused by ALA+SFC.

336

337 **Fig 5. MKN45 proliferation was inhibited by ALA+SFC and it was canceled by addition of a ROS**
338 **scavenger Tiron.** (A) MKN45 cell numbers estimated by trypan blue dye exclusion assay on day 0, 2, 4.
339 (B) MKN45 cells were incubated with 1 mM ALA, 0.5 mM SFC and 100 μ M Tiron for 24 hours and
340 intracellular ROS levels were detected using a DCFH-DA based method. The graph shows relative
341 fluorescence intensity of DCF. (C) MKN45 were cultured with 1 mM ALA, 0.5 mM SFC, and 100 μ M
342 Tiron for 24 hours and growth assay was performed similar to that in Fig 5a. Values are means \pm SD, n =

343 3, Asterisk indicates a significant difference analyzed by Dunnett's test (A) and Tukey-Kramer's test (B,
344 C) (*; $p < 0.05$, **; $p < 0.01$).

345

346 Thus, ALA+SFC were suggested to promote heme synthesis, enhance aerobic respiration,
347 generate ROS, and inhibit proliferation of cancer cells.

348 **Discussion**

349 In this study, we evaluated energy metabolism in cancer cells to better understand the
350 relationship between heme synthesis and the Warburg effect. Indicators of glycolysis namely, GLUT1
351 expression, uptake of 2-NBDG, lactic acid production, and pH of culture media were significantly up-
352 regulated under hypoxic conditions. Further, heme metabolism and intracellular heme concentration was
353 significantly reduced under hypoxic conditions. Thus, a negative correlation between heme synthesis and
354 glycolysis was suggested based on hypoxia-induced acceleration of the glycolytic system and deceleration
355 of heme synthesis in gastric cancer cell lines. The effect of ALA+SFC and SA, up- and down-regulators
356 of heme metabolism, respectively, on COX and mitochondrial DNA suggested that promotion of heme
357 synthesis led to a shift in energetic metabolism from glycolysis to oxidative phosphorylation by enhancing
358 COX expression and activity of cancer cells. This led to elimination of the Warburg effect. Finally, gastric
359 cancer cells exposed to ALA+SFC showed significantly reduced cell growth caused by increased
360 intracellular ROS generation.

361 ALA is a naturally occurring amino acid synthesized *in vivo* from succinyl CoA and glycine and
362 is metabolized to porphyrin in multiple steps occurring in the cytoplasm and mitochondria. Ferrochelatase
363 catalyzes the insertion of ferrous iron into PpIX and is thereby the terminal step of heme synthesis and
364 conversion of PpIX to heme. Similarly, tumor cells are known to accumulate PpIX under low activity of

365 ferrochelatase [13,14]. This phenomenon allows photodynamic diagnosis using ALA [34,35]. Earlier, we
366 reported that the membrane transporter ABCB6, which is mainly expressed on mitochondrial membrane
367 for transporting CPgenIII from cytosol into mitochondria, is polarized on the cytoplasmic membrane under
368 hypoxic conditions. This results in the extracellular export of porphyrins [25]. Our results (Fig 2AB) are
369 consistent with this mechanism.

370 Earlier, we have shown that COX activity and ATP concentration was strongly up-regulated in
371 mouse liver after ALA was injected [22]. In this study, the human gastric cancer cell line MKN45 showed
372 increased expression and activity of COX in presence of ALA+SFC. Also, ALA+SFC act as heme
373 substrates and lead to up-regulation of COX in both normal and cancer cells. This is supported by that the
374 inhibitor of heme synthesis, SA, suppressed COX up-regulation and elevated glycolysis (Fig 3, 4).

375 Most cancer cells suppress mitochondrial aerobic respiration and synthesize ATP necessary for
376 proliferation and metastasis by enhancing the glycolytic system. Thus, cancer cells require a large amount
377 of glucose. This was advocated by Warburg in 1924 and became widely recognized as the Warburg effect
378 [1]. Glycolysis is not efficient for ATP production but forceful for other substance productivity such as
379 nucleic acids and lipids [36–38]. Therefore, glycolysis is better than oxidative phosphorylation for rapid
380 proliferation. Several attempts have been made to treat cancer cells by focusing on this characteristic

381 metabolic adaptation of cancer cells [39–41]. Glucose derivatives such as fluorodeoxyglucose (FDG) and
382 2-deoxyglucose (2-DG) are used for diagnosis and treatment of cancer [41–43].

383 Attempts have been made to treat cancer by inducing ROS production from mitochondrial
384 respiration such as dichloroacetate (DCA). The conversion of pyruvate to acetyl CoA by pyruvate
385 dehydrogenase (PDH) is the rate-limiting step in glycolysis. DCA activates PDH and inhibits lactic acid
386 synthesis and is therefore used as an oral therapeutic agent for mitochondrial diseases, including lactic
387 acidosis. It has reported that DCA restores PDH activity of cancer cells and activates oxidative
388 phosphorylation and consequently induces apoptosis [19,21]. Besides, it is reported that the small
389 molecule ATN-224, which is an inhibitor of superoxide dismutase 1 (SOD1), leads to reduction of lung
390 tumor volume *in vivo* and ROS-dependent cell death *in vitro*. Thus, controlling ROS can be effective in
391 cancer treatment.

392 It is known that superoxide anion radicals are generated by trapping electrons that leak out of
393 oxygen molecules when the mitochondrial membrane potential becomes unstable owing to changes in the
394 activity of ETS [44,45]. The activation of COX in MKN45 cells by ALA+SFC (Fig 4) indicated that the
395 leakage of superoxide anions from mitochondria most probably led to increased ROS (Fig 5). We used
396 Tiron, an analog of vitamin E and a radical scavenger, as a ROS scavenger [32,33]. Tiron reduced ROS
397 levels and showed recovery of cell proliferation (Fig 5). Taken together, it suggested that ALA+SFC

398 enhanced mitochondrial activity and leakage of superoxide anion radicals followed by an induction in
399 cancer cell death.

400 To the best of our knowledge, there is no comprehensive study on the relationship between heme
401 synthesis and the Warburg effect. This study provides a novel insight into the complex metabolism of
402 cancer cells and presents a promising new therapeutic strategy for treating cancer. Further studies are
403 required to reveal the molecular mechanism of ALA combined with the Warburg effect toward disruption
404 and elimination of cancer cells.

405 Reference

- 406 1. WARBURG O. On respiratory impairment in cancer cells. *Science*. 1956;124: 269–70.
- 407 2. Semenza GL. Targeting HIF-1 for cancer therapy. *Nat Rev Cancer*. 2003;3: 721–32.
- 408 doi:10.1038/nrc1187
- 409 3. THOMLINSON RH, GRAY LH. The histological structure of some human lung cancers and the
- 410 possible implications for radiotherapy. *Br J Cancer*. 1955;9: 539–49.
- 411 4. Nordmark M, Bentzen SM, Overgaard J. Measurement of human tumour oxygenation status by a
- 412 polarographic needle electrode. An analysis of inter- and intratumour heterogeneity. *Acta Oncol*.
- 413 1994;33: 383–9.
- 414 5. Kim J, Tchernyshyov I, Semenza GL, Dang C V. HIF-1-mediated expression of pyruvate
- 415 dehydrogenase kinase: a metabolic switch required for cellular adaptation to hypoxia. *Cell Metab*.
- 416 2006;3: 177–85. doi:10.1016/j.cmet.2006.02.002
- 417 6. Younes M, Lechago L V, Somoano JR, Mosharaf M, Lechago J. Wide expression of the human
- 418 erythrocyte glucose transporter Glut1 in human cancers. *Cancer Res*. 1996;56: 1164–7.
- 419 7. Iyer N V, Kotch LE, Agani F, Leung SW, Laughner E, Wenger RH, et al. Cellular and
- 420 developmental control of O₂ homeostasis by hypoxia-inducible factor 1 alpha. *Genes Dev*.
- 421 1998;12: 149–62.

- 422 8. Semenza GL. HIF-1 mediates metabolic responses to intratumoral hypoxia and oncogenic
423 mutations. *J Clin Invest.* 2013;123. doi:10.1172/JCI67230
- 424 9. Courtney R, Ngo DC, Malik N, Ververis K, Tortorella SM, Karagiannis TC. Cancer metabolism
425 and the Warburg effect: the role of HIF-1 and PI3K. *Mol Biol Rep.* 2015;42: 841–51.
426 doi:10.1007/s11033-015-3858-x
- 427 10. Ishizuka M, Abe F, Sano Y, Takahashi K, Inoue K, Nakajima M, et al. Novel development of 5-
428 aminolevulinic acid (ALA) in cancer diagnoses and therapy. *Int Immunopharmacol.* 2011;11:
429 358–365. doi:10.1016/j.intimp.2010.11.029
- 430 11. Woodard SI, Dailey HA. Multiple regulatory steps in erythroid heme biosynthesis. *Arch Biochem*
431 *Biophys.* 2000;384: 375–8. doi:10.1006/abbi.2000.2069
- 432 12. Krishnamurthy P, Xie T, Schuetz JD. The role of transporters in cellular heme and porphyrin
433 homeostasis. *Pharmacol Ther.* 2007;114: 345–58. doi:10.1016/j.pharmthera.2007.02.001
- 434 13. Ohgari Y, Nakayasu Y, Kitajima S, Sawamoto M, Mori H, Shimokawa O, et al. Mechanisms
435 involved in delta-aminolevulinic acid (ALA)-induced photosensitivity of tumor cells: relation of
436 ferrochelatase and uptake of ALA to the accumulation of protoporphyrin. *Biochem Pharmacol.*
437 2005;71: 42–9. doi:10.1016/j.bcp.2005.10.019
- 438 14. Kemmner W, Wan K, Rüttinger S, Ebert B, Macdonald R, Klamm U, et al. Silencing of human

- 439 ferrochelatase causes abundant protoporphyrin-IX accumulation in colon cancer. *FASEB J.*
440 2008;22: 500–9. doi:10.1096/fj.07-8888com
- 441 15. FALK JE, PORRA RJ, BROWN A, MOSS F, LARMINIE HE. Effect of oxygen tension on haem
442 and porphyrin biosynthesis. *Nature.* 1959;184: 1217–9.
- 443 16. Georgakoudi I, Keng PC, Foster TH. Hypoxia significantly reduces aminolaevulinic acid-induced
444 protoporphyrin IX synthesis in EMT6 cells. *Br J Cancer.* 1999;79: 1372–7.
445 doi:10.1038/sj.bjc.6690220
- 446 17. Chan SY, Zhang Y-Y, Hemann C, Mahoney CE, Zweier JL, Loscalzo J. MicroRNA-210 controls
447 mitochondrial metabolism during hypoxia by repressing the iron-sulfur cluster assembly proteins
448 ISCU1/2. *Cell Metab.* 2009;10: 273–84. doi:10.1016/j.cmet.2009.08.015
- 449 18. Zhang Y, Furuyama K, Kaneko K, Ding Y, Ogawa K, Yoshizawa M, et al. Hypoxia reduces the
450 expression of heme oxygenase-2 in various types of human cell lines. A possible strategy for the
451 maintenance of intracellular heme level. *FEBS J.* 2006;273: 3136–47. doi:10.1111/j.1742-
452 4658.2006.05319.x
- 453 19. Michelakis ED, Webster L, Mackey JR. Dichloroacetate (DCA) as a potential metabolic-targeting
454 therapy for cancer. *Br J Cancer.* 2008;99: 989–94. doi:10.1038/sj.bjc.6604554
- 455 20. Sutendra G, Dromparis P, Kinnaird A, Stenson TH, Haromy A, Parker JMR, et al. Mitochondrial

- 456 activation by inhibition of PDKII suppresses HIF1a signaling and angiogenesis in cancer.
457 *Oncogene*. 2013;32: 1638–50. doi:10.1038/onc.2012.198
- 458 21. Bonnet S, Archer SL, Allalunis-Turner J, Haromy A, Beaulieu C, Thompson R, et al. A
459 mitochondria-K⁺ channel axis is suppressed in cancer and its normalization promotes apoptosis
460 and inhibits cancer growth. *Cancer Cell*. 2007;11: 37–51. doi:10.1016/j.ccr.2006.10.020
- 461 22. Ogura S-I, Maruyama K, Hagiya Y, Sugiyama Y, Tsuchiya K, Takahashi K, et al. The effect of 5-
462 aminolevulinic acid on cytochrome c oxidase activity in mouse liver. *BMC Res Notes*. 2011;4: 66.
463 doi:10.1186/1756-0500-4-66
- 464 23. Sugiyama Y, Hagiya Y, Nakajima M, Ishizuka M, Tanaka T, Ogura S-I. The heme precursor 5-
465 aminolevulinic acid disrupts the Warburg effect in tumor cells and induces caspase-dependent
466 apoptosis. *Oncol Rep*. 31: 1282–6. doi:10.3892/or.2013.2945
- 467 24. Hagiya Y, Adachi T, Ogura S, An R, Tamura A, Nakagawa H, et al. Nrf2-dependent induction of
468 human ABC transporter ABCG2 and heme oxygenase-1 in HepG2 cells by photoactivation of
469 porphyrins: biochemical implications for cancer cell response to photodynamic therapy. *J Exp*
470 *Ther Oncol*. 2008;7: 153–67.
- 471 25. Matsumoto K, Hagiya Y, Endo Y, Nakajima M, Ishizuka M, Tanaka T, et al. Effects of plasma
472 membrane ABCB6 on 5-aminolevulinic acid (ALA)-induced porphyrin accumulation in vitro:

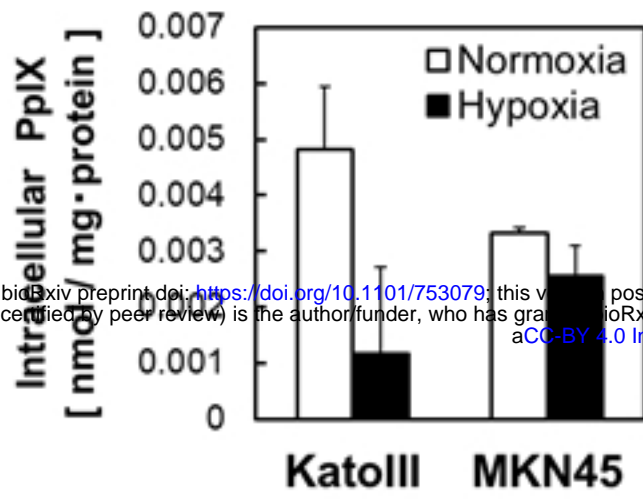
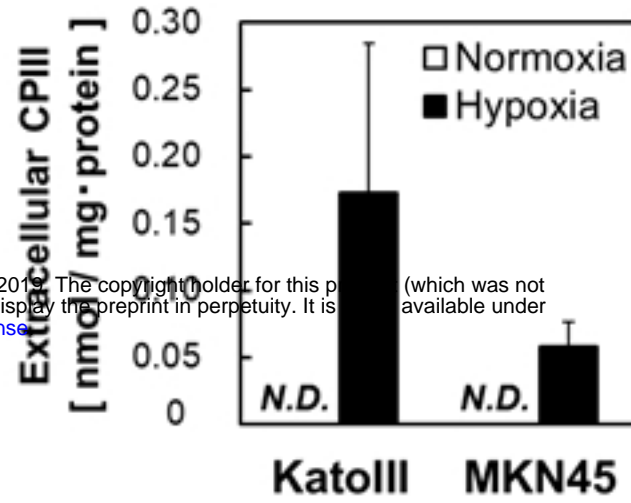
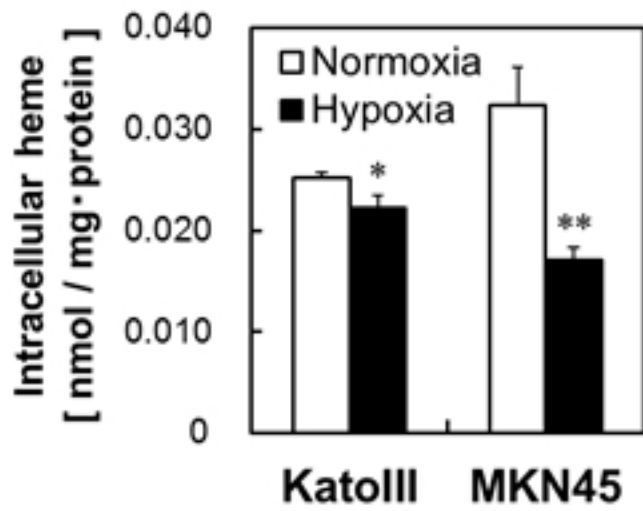
- 473 tumor cell response to hypoxia. *Photodiagnosis Photodyn Ther.* 2015;12: 45–51.
474 doi:10.1016/j.pdpdt.2014.12.008
- 475 26. Berry EA, Trumpower BL. Simultaneous determination of hemes a, b, and c from pyridine
476 hemochrome spectra. *Anal Biochem.* 1987;161: 1–15.
- 477 27. Kadenbach B, Hüttemann M, Arnold S, Lee I, Bender E. Mitochondrial energy metabolism is
478 regulated via nuclear-coded subunits of cytochrome c oxidase. *Free Radic Biol Med.* 2000;29:
479 211–21.
- 480 28. Arnold S. The power of life—Cytochrome c oxidase takes center stage in metabolic control, cell
481 signalling and survival. *Mitochondrion.* 2012;12: 46–56. doi:10.1016/j.mito.2011.05.003
- 482 29. Tsukihara T, Aoyama H, Yamashita E, Tomizaki T, Yamaguchi H, Shinzawa-Itoh K, et al. The
483 whole structure of the 13-subunit oxidized cytochrome c oxidase at 2.8 Å. *Science.* 1996;272:
484 1136–44.
- 485 30. Murphy MP. How mitochondria produce reactive oxygen species. *Biochem J.* 2009;417: 1–13.
486 doi:10.1042/BJ20081386
- 487 31. Sullivan LB, Chandel NS. Mitochondrial reactive oxygen species and cancer. *Cancer Metab.*
488 2014;2: 17. doi:10.1186/2049-3002-2-17
- 489 32. Taiwo FA. Mechanism of tiron as scavenger of superoxide ions and free electrons. *J Spectrosc.*

- 490 22: 491–498. doi:10.3233/SPE-2008-0362
- 491 33. Ledenev AN, Konstantinov AA, Popova E, Ruuge EK. A simple assay of the superoxide
492 generation rate with Tiron as an EPR-visible radical scavenger. *Biochem Int.* 1986;13: 391–6.
- 493 34. Stummer W, Pichlmeier U, Meinel T, Wiestler OD, Zanella F, Reulen H-J, et al. Fluorescence-
494 guided surgery with 5-aminolevulinic acid for resection of malignant glioma: a randomised
495 controlled multicentre phase III trial. *Lancet Oncol.* 2006;7: 392–401. doi:10.1016/S1470-
496 2045(06)70665-9
- 497 35. Krammer B, Plaetzer K. ALA and its clinical impact, from bench to bedside. *Photochem Photobiol*
498 *Sci.* 2008;7: 283–289. doi:10.1039/B712847A
- 499 36. Vander Heiden MG, Cantley LC, Thompson CB. Understanding the Warburg effect: the metabolic
500 requirements of cell proliferation. *Science.* 2009;324: 1029–33. doi:10.1126/science.1160809
- 501 37. DeBerardinis RJ, Mancuso A, Daikhin E, Nissim I, Yudkoff M, Wehrli S, et al. Beyond aerobic
502 glycolysis: transformed cells can engage in glutamine metabolism that exceeds the requirement
503 for protein and nucleotide synthesis. *Proc Natl Acad Sci U S A.* 2007;104: 19345–50.
504 doi:10.1073/pnas.0709747104
- 505 38. Vander Heiden MG, Locasale JW, Swanson KD, Sharfi H, Heffron GJ, Amador-Noguez D, et al.
506 Evidence for an alternative glycolytic pathway in rapidly proliferating cells. *Science.* 2010;329:

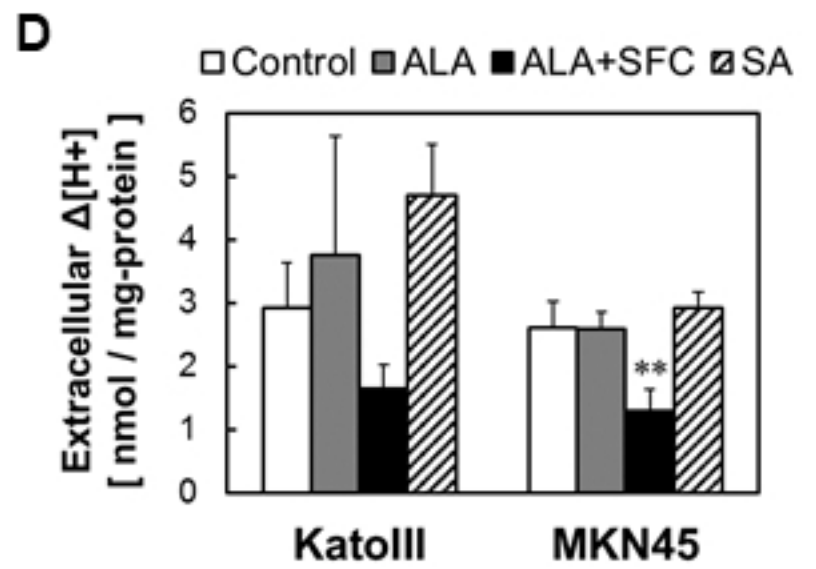
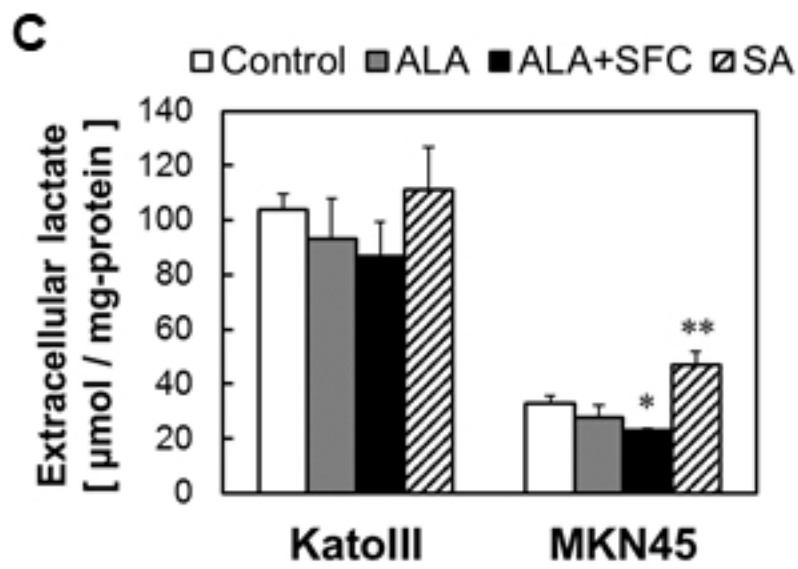
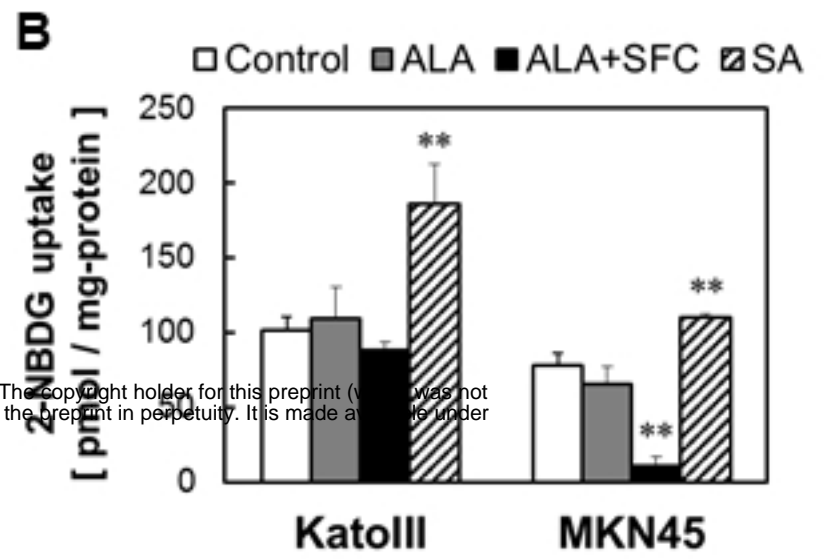
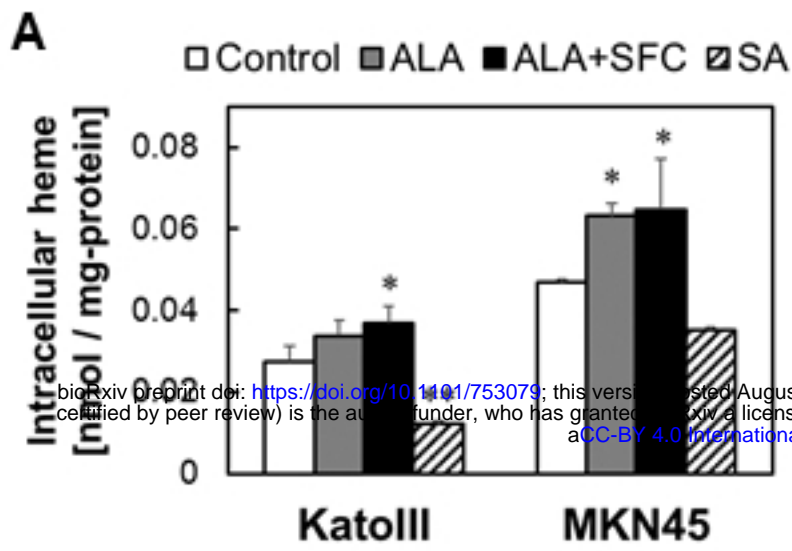
- 507 1492–9. doi:10.1126/science.1188015
- 508 39. Tennant DA, Durán R V, Gottlieb E. Targeting metabolic transformation for cancer therapy. Nat
509 Rev Cancer. 2010;10: 267–77. doi:10.1038/nrc2817
- 510 40. Zhao Y, Butler EB, Tan M. Targeting cellular metabolism to improve cancer therapeutics. Cell
511 Death Dis. 2013;4: e532. doi:10.1038/cddis.2013.60
- 512 41. Pelicano H, Martin DS, Xu R-H, Huang P. Glycolysis inhibition for anticancer treatment.
513 Oncogene. 2006;25: 4633–46. doi:10.1038/sj.onc.1209597
- 514 42. Mankoff DA, Eary JF, Link JM, Muzi M, Rajendran JG, Spence AM, et al. Tumor-specific
515 positron emission tomography imaging in patients: [18F] fluorodeoxyglucose and beyond. Clin
516 Cancer Res. 2007;13: 3460–9. doi:10.1158/1078-0432.CCR-07-0074
- 517 43. Cheng G, Zielonka J, Dranka BP, McAllister D, Mackinnon AC, Joseph J, et al. Mitochondria-
518 targeted drugs synergize with 2-deoxyglucose to trigger breast cancer cell death. Cancer Res.
519 2012;72: 2634–44. doi:10.1158/0008-5472.CAN-11-3928
- 520 44. Mailloux RJ, Harper M-E. Uncoupling proteins and the control of mitochondrial reactive oxygen
521 species production. Free Radic Biol Med. 2011;51: 1106–1115.
522 doi:10.1016/j.freeradbiomed.2011.06.022
- 523 45. Turrens JF. Mitochondrial formation of reactive oxygen species. J Physiol. 2003;552: 335–44.

524 doi:10.1113/jphysiol.2003.049478

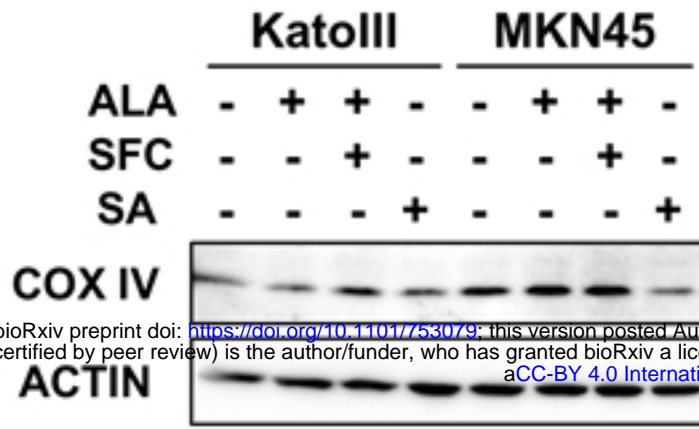
525

A**B****C**

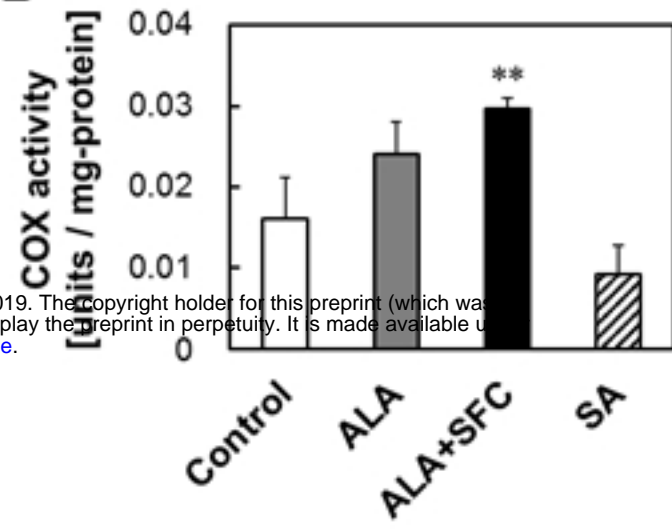
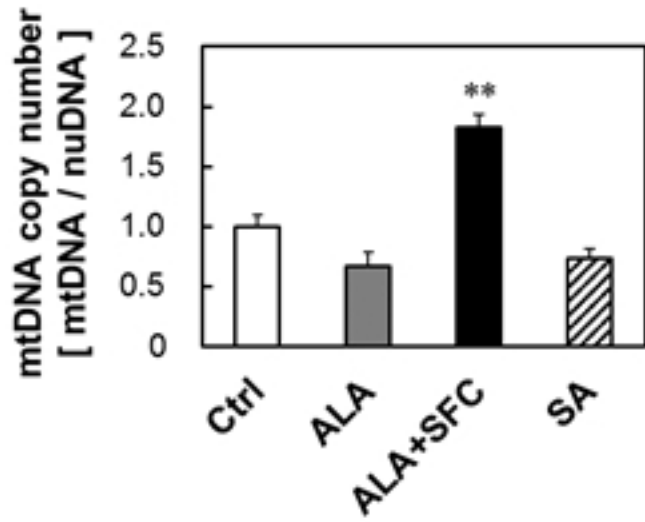
bioRxiv preprint doi: <https://doi.org/10.1101/753079>; this version posted August 30, 2019. The copyright holder for this preprint (which was not certified by peer review) is the author/funder, who has granted bioRxiv a license to display the preprint in perpetuity. It is made available under aCC-BY 4.0 International license.

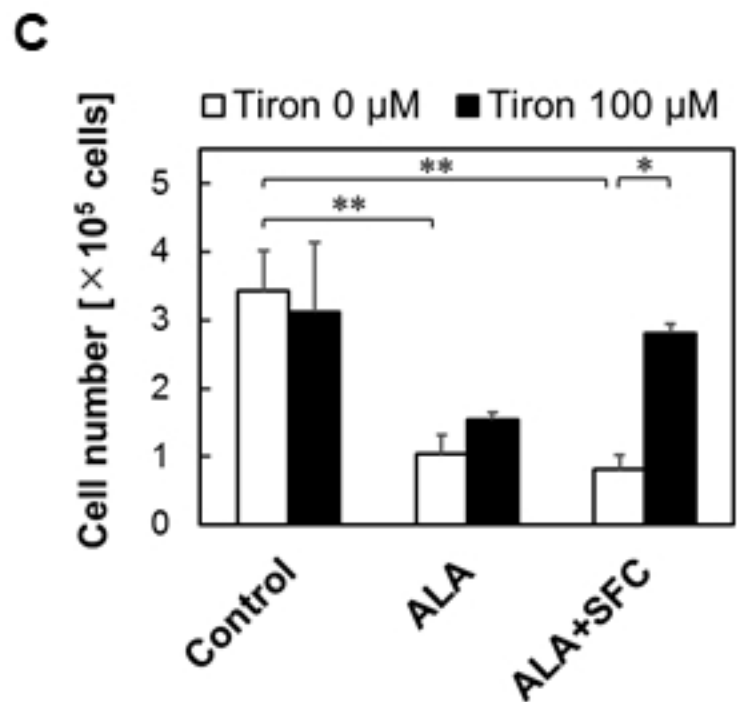
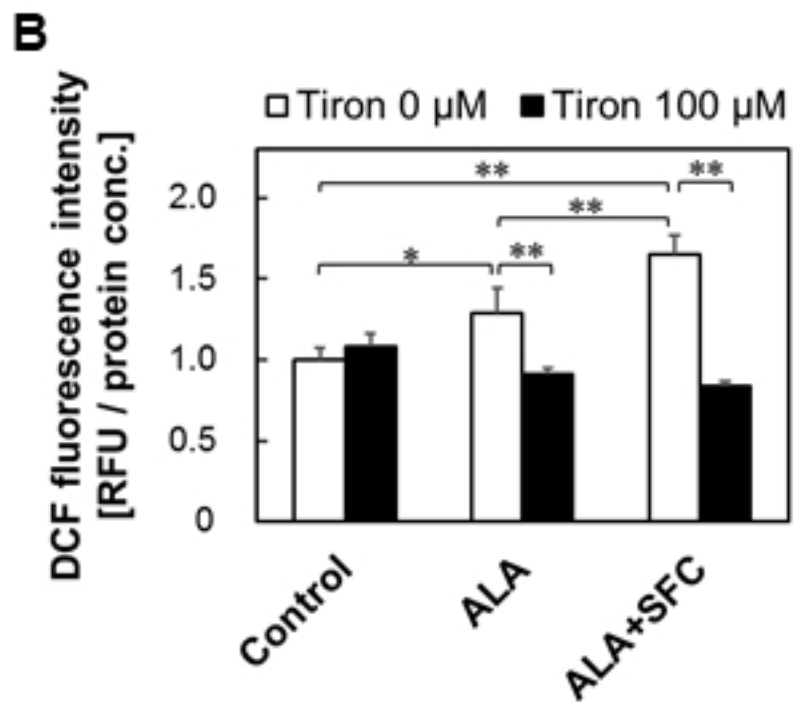
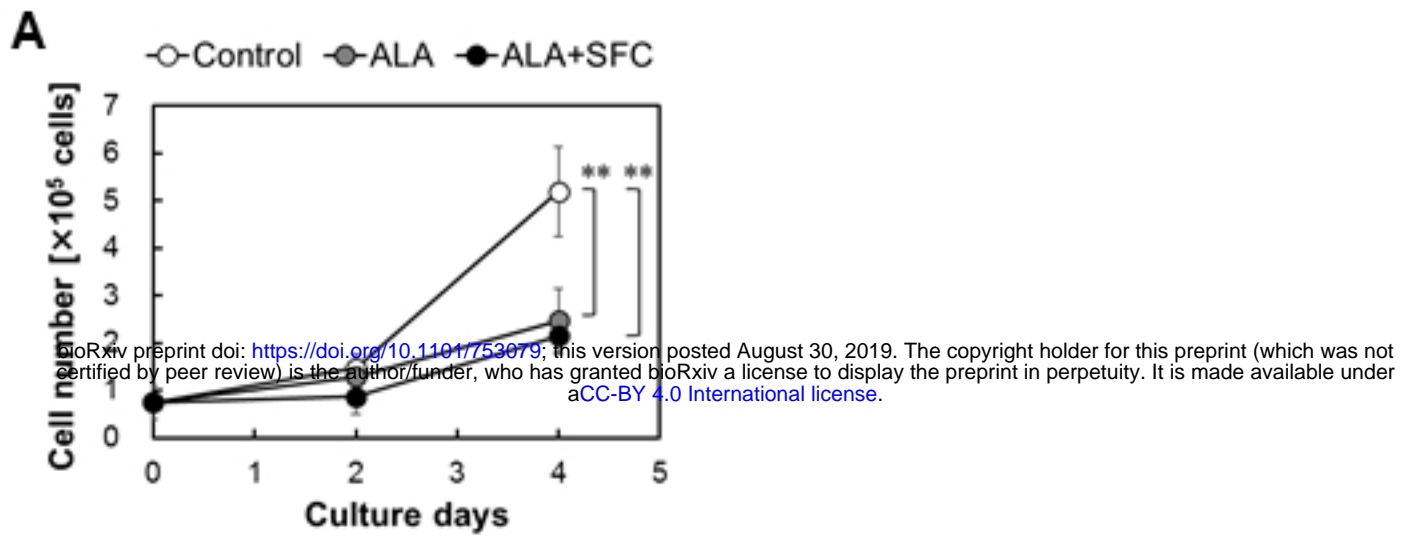


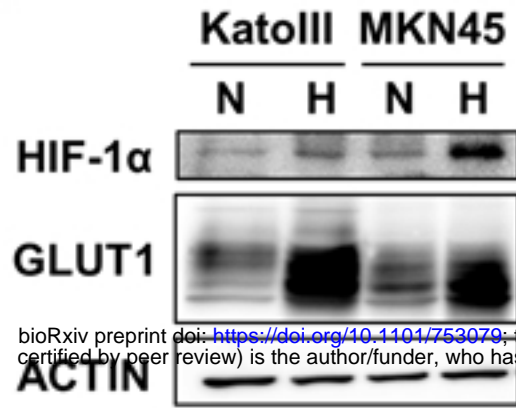
bioRxiv preprint doi: <https://doi.org/10.1101/753079>; this version posted August 30, 2019. The copyright holder for this preprint (which was not certified by peer review) is the author/funder, who has granted bioRxiv a license to display the preprint in perpetuity. It is made available under aCC-BY 4.0 International license.

A

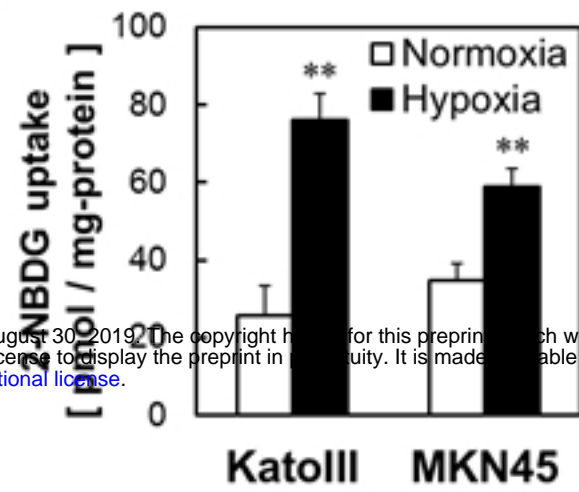
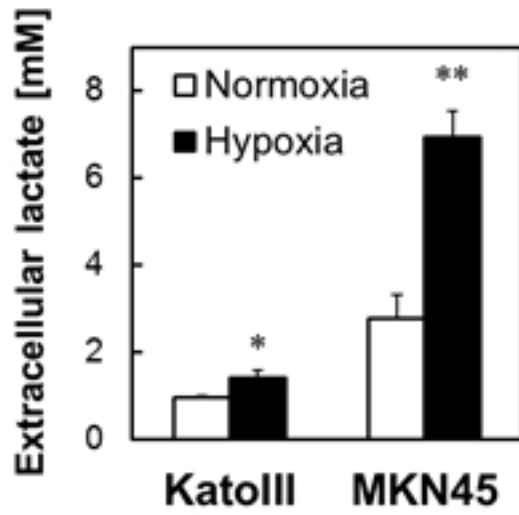
bioRxiv preprint doi: <https://doi.org/10.1101/753079>; this version posted August 30, 2019. The copyright holder for this preprint (which was certified by peer review) is the author/funder, who has granted bioRxiv a license to display the preprint in perpetuity. It is made available under aCC-BY 4.0 International license.

B**C**



A

bioRxiv preprint doi: <https://doi.org/10.1101/753079>; this version posted August 30, 2019. The copyright holder for this preprint (which was not certified by peer review) is the author/funder, who has granted bioRxiv a license to display the preprint in perpetuity. It is made available under aCC-BY 4.0 International license.

B**C****D**